W79A Session C25, WCRP, Oct. 26

Intra-seasonal oscillation and its control over tropical cyclones in the high resolution global atmospheric models

Kazuyoshi Oouchi1, Masaki Satoh1,2, Tomoe Nasuno1, Hiroshi Taniguchi3, Yohei Yamada1, Hirofumi Tomita1,4, Chihiro Kodama1, James Kinter III5, Deepthi Achuthavarier5, Julia Manganello5

1. JAMSTEC, 2. Atmosphere-Ocean Research Institute, the University of Tokyo, 3. International Pacific Research Center, SOEST, University of Hawaii at Manoa, 4. Advanced Institute for Computational Science/RIKEN, 5. Center for Ocean-Land-Atmosphere Studies,

Background

Origin of Project (Dr. Jim Kinter)

- The World Modeling Summit (WMS) in May 2008 at ECMWF called for revolution in climate modeling to more rapidly advance improvement in climate model resolution, accuracy and reliability
- The WMS recommended petascale supercomputers dedicated to climate modeling at at least 3 international facilities
  - Dedicated petascale machines are needed to provide enough computational capability and a controlled environment to support long runs and the management and analysis of very large (petabyte) data sets
- The U.S. National Science Foundation, recognizing the importance of the problem, realized that a resource (Athena supercomputer) was available to meet the challenge of the World Modeling Summit and offered to dedicate the Athena supercomputer over a six-month period in 2009-2010
- An international collaboration was formed among groups in the U.S., Japan and the U.K. to use Athena to take up the challenge

- **Hypothesis**: Exploring high spatial resolution and process-resolving models can dramatically alter simulation of climate
- Two state-of-the-art global AGCMs at the **highest possible spatial resolution**
- **Dedicated supercomputer** at NICS for Oct'09 – Mar'10
- Long term - **model output data will be invaluable** for large community of climate scientists (unprecedented resolution and simulation duration) and computational scientists (lessons learned from running dedicated production at nearly petascale)

Supercomputer

- **Athena: Cray XT4 - 4512 quad-core Opteron nodes (18048)**
  - **#30 on Top500 list (November 2009) – dedicated Oct'09 – Mar'10**

Models and Experimental Designs (ECMWF-IFS, NICAM)

ECMWF–IFS

Refs. Bechtold et al. 2008 , Jung et al. 2010.

European Centre for Medium-range Weather Forecasts Comprehensive Earth-System Model

Horizontal resolution: T2047 (~ 10 km)
Vertical layers : 91 layers
Cumulus scheme : Tiedtke (1989)

SST and sea ice : weekly 1°×1° NCEP Reynolds OI dataset (Reynolds et al. 2002).

NICAM

Refs. Satoh et al. 2008, Tomita and Satoh 2004

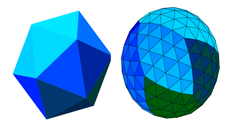

Non-hydrostatic Icosahedral Atmosheric Model (Fully compressible non-hydrostatic system)

Horizontal resolution: ~ 7km
Vertical layers : 40 layers
Cumulus scheme : None
Cloud microphysics : NSW 6 (Tomita 2008)
- 6 categories of water (1 moment bulk)
Turbulences/shallow clouds: MYNN2 (Noda et al. 2010, Nakanishi and Niino 2004)
Radiation : MSTRNX (Sekiguchi and Nakajima, 2008)
Land-surface: MATSIRO (Takata, 2003)
SST and sea ice : weekly NCEP Reynolds OI dataset

Time Integration Period

- **May 21 – August 31 for 2001-2002, 2004-2009 boreal summer over 8 years**

Results – Intra-seasonal Oscillation (ISO) in the monsoon region

Monthly mean zonal wind 850 hPa

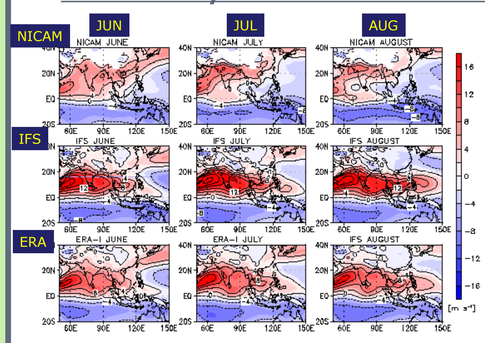

Fig. 1 The 8-year averaged monthly mean zonal wind at 850 hPa in NICAM (top) and IFS (middle) simulations in comparison with ERA–Interim (bottom).

- The Somali jet, a well-known characteristic of the boreal summer monsoon circulation in the western Indian Ocean, is pronounced.

- Westerlies prevail along 10° -15° N, and extend eastward associated with the evolution of the monsoon (ERA -Interim) .

- The horizontal pattern and the seasonal march of the monsoon are well reproduced by IFS, although the magnitude of the westerlies is overpredicted (middle). In contrast, NICAM fails to reproduce the eastward migration of westerlies and under-predicts the Somali jet (top).

Time series of precipitation / zonal wind anomaly 850 hPa

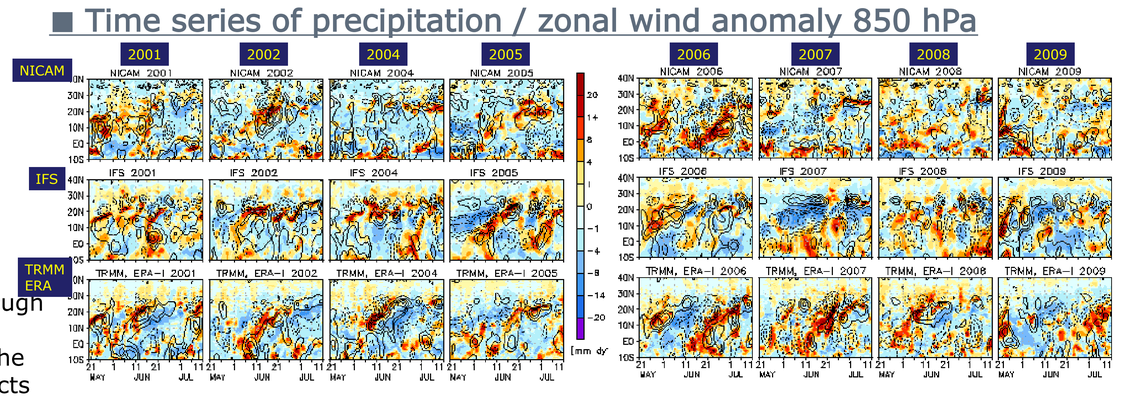

Fig.4 Time-latitude sections of anomalous 60-90E average surface precipitation (color) and zonal wind at 850 hPa (contour lines in the initial 52 days of NICAM (top) and IFS (middle) simulations in comparison with TRMM–3B42 and ERA–Interim data (bottom). The anomalies from the 8-year average (Fig. 2) are plotted. Contour intervals for zonal wind are 2 m s^{-1}(solid: positive, broken: negative). Zero contour lines are omitted.

Time series of precipitation / zonal wind 850 hPa

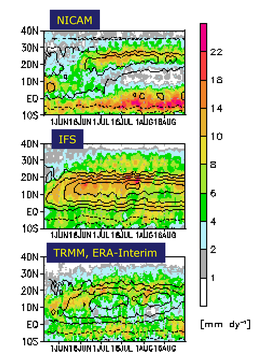

-The maximum westerlies and precipitation are located at 5° -10° N during May, shift northward in early June, and stay around 15° -20° N through June to August (bottom).

- Both simulations capture the intensification and northward displacement of maximum westerly and precipitation in early June except for some biases in the excessive peak intensity (~15° N) in IFS, and weaker intensity and peak latitudes occurring 5-10 degrees northward in NICAM.

Fig.2 Time-latitude sections of the 8-year 60-90E averaged precipitation (color) and zonal wind at 850 hPa (contour lines) in NICAM (top) and IFS (middle) simulations in comparison with TRMM–3B42 and ERA–Interim (bottom). Contour intervals for zonal wind are 4 m s^{-1} (solid: positive, broken: negative). Zero contour lines are omitted.

Time series of Indian Monsoon Index (Wang et al. 2001) and correlation between model and observation

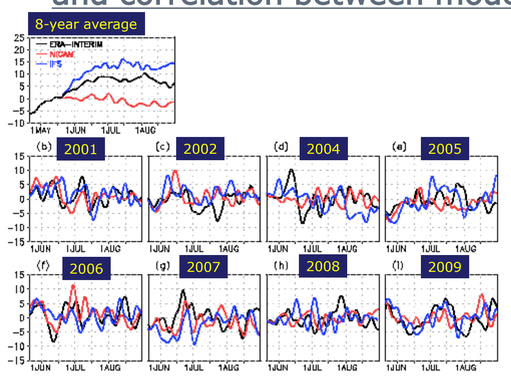

Fig.3 Time series of the Indian Monsoon Index (Wang et al. 2001) for NICAM and IFS simulations and ERA–Interim data. (a) The 8-year average and (b)–(i) anomaly from the average are plotted. 5-day running mean is operated.

	NICAM			IFS		
year	1st	2nd	3rd	1st	2nd	3rd
2001	0.730	0.663	-0.287	-0.515	0.467	-0.138
2002	0.879	-0.145	-0.546	0.531	0.673	-0.058
2004	0.384	0.304	0.063	0.163	-0.572	0.093
2005	0.877	-0.322	-0.655	0.493	0.044	0.263
2006	0.911	0.006	-0.081	0.653	0.402	0.393
2007	0.269	0.404	0.242	0.201	0.248	0.672
2008	0.294	0.137	-0.141	-0.226	-0.688	-0.095
2009	0.847	0.510	-0.205	0.836	0.712	0.152
average	0.648	0.194	-0.201	0.267	0.160	0.160
stdev	0.264	0.315	0.277	0.427	0.499	0.258

Table 1. Correlation coefficients of the time series of anomalous IMI (Fig. 3b-i) in NICAM and IFS simulations against that in ERA-Interim for the 1st, 2nd ,and 3rd month of simulation period. 8-year averages and standard deviation are also presented for the three periods.

- Fluctuations with time scales of 2-4 weeks, which are referred to as ISO, are evident in all years in ERA Interim. ISOs are masked out by the 8-year average (Fig. 3a) because the timing of the ISOs are not exactly the same in every year. However, both IFS and NICAM reproduce the ISO in the first month of simulation relatively well.

- Correlation coefficients of the time series of IMI between simulations and ERA-Interim (Fig. 3) for the first, second, and third month of integration for each year are summarized in Table 1. NICAM reproduce the ISO in the first month of simulation better than in the latter two months, with correlation coefficients exceeding 0.8 in some years (e.g., 2002, 2006 and 2009), although statistical significance are not necessarily guaranteed by the eight samples. In the IFS simulations coefficients in the first and second month are equivalent and decreasing in the third month.

Results – Madden-Julian oscillation and tropical cyclogenesis

Hovmoller diagram : composite of velocity potential anomaly 200 hPa (15S– 15N)

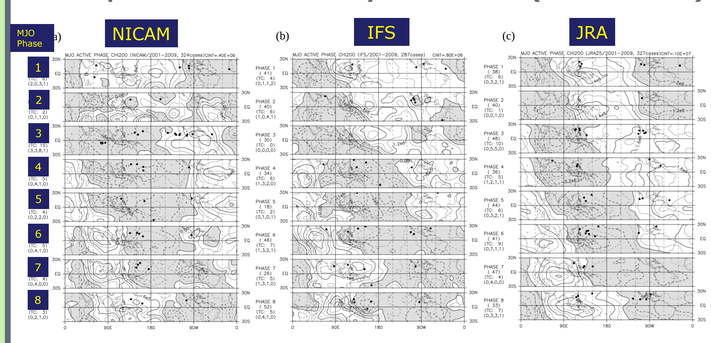

Fig. 5 Composite 200 hPa velocity potential anomalies (contours; shading for negative values and solid contours for positive values) for each phase of the MJO defined in Fig. 8 for the MJO-active period defined in the same method as Taniguchi et al. (2010) for 21 May to 31 July 2001 to 2009 except 2003. Left (a), center (b), and right (c) panels show the results of the NICAM and IFS simulations, and the observations (re-analysis) by JRA/JCDAS analysis, respectively. The total numbers of selected dates for the MJO-active period for figures (a), (b), and (c) are 318, 287, and 336 days, respectively. Contour intervals of (a), (b), and (c) are 0.5 x 10^6, 0.8 x 10^6, and 1.0 x 10^6 (m^2/s), respectively. Also plotted are the locations of TC genesis in each phase (solid circles) during the same period.

- How the two models simulate the relationship between MJO and TCs are examined. The distinct eastward propagation of convective anomalies associated with MJO is evident in all panels. For NICAM (Fig. 5a), the area of convective anomalies in phases 3, 4, and 5 (active convection over the Indian Ocean to the maritime continent) is larger than in the observations (Fig. 5c), while in the area in phases 2 and 7 (active convection over the Atlantic Ocean) is smaller than that in the observations. Presumably, these features are related to more active/inactive convection in NICAM compared to the observations over the regions of the Indian Ocean to the maritime continent /Atlantic Ocean, respectively.

- On the other hand, for IFS (Fig. 5b), the area of convective anomalies in phases 1, 2, 7, and 8 is smaller in the region of the Atlantic Ocean to the African continent than that of the observations. This is probably due to inactive convection in IFS compared to the observations in the western hemisphere.

Tropical cyclogenesis frequency with respect to MJO phases

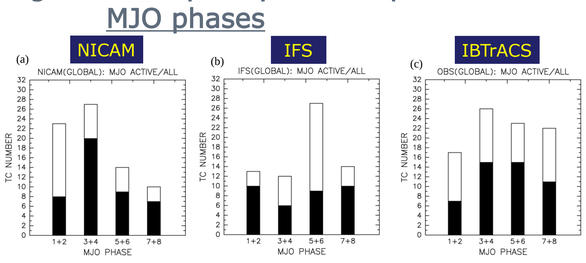

Fig. 6 The occurrence of TC genesis in each phase of the MJO during the period of 2001 to 2009 except 2003. Solid and open square bars indicate the occurrence for the MJO-active period, shown by solid circles in Fig. 14, and the occurrence for the whole period of MJO, respectively. The left (a), center (b), and right (c) columns show the results of the NICAM and IFS simulations, and the observations by IBTrACS, respectively.

- The ratio of the cyclogenesis frequency in the MJO-active period to that of the whole period indicates that the contribution of MJO to cyclogenesis is prominent in the sets of phases 3+4 and 5+6 as a whole in Fig. 6c, and this characteristic is well captured in NICAM.

Summary and Future Issues

- The current skill of the Athena models in simulating intra-seasonal oscillations (MJO and ISO) in the tropical and monsoon region is overall encouraging. The performance of NICAM shown in the case studies of MJO (Miura et al. 2007) and monsoon-related ISO (Oouchi et al. 2009) are proven to be robust in multi-season runs.

- These are the first long-term runs (3 months x 8 years) for 7-km mesh NICAM without special tuning of the physical packages – with improved NICAM, detailed understanding of the interactions across the scales ranging from meso-to-planetary phenomena would be obtained when we have more computational resources at hand.

- K-computer (Kobe, Japan) will be starting its operation next year, and then 7-km mesh NICAM will be run over more than several years to investigate statistics of these intra-seasonal phenomena – pursuing the feasibility of extended forecasts for tropical to mid-latitude regions.

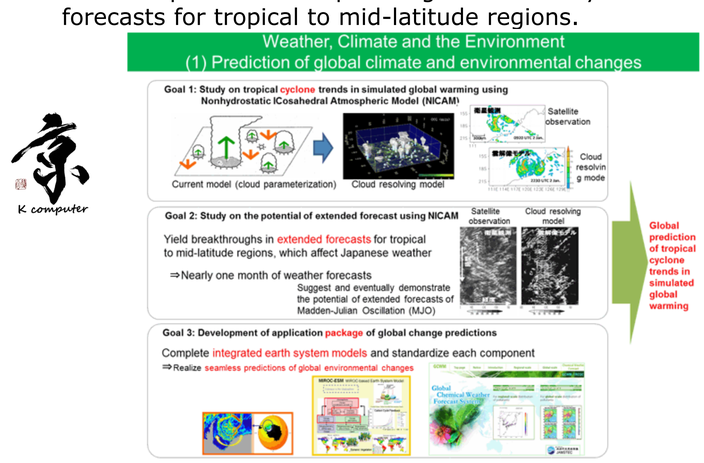

Questions and comments are welcome
Kazuyoshi Oouchi, E-mail: k-ouchi@jamstec.go.jp

References

- Bechtold et al. 2008, QJRM, 134, 1337.
- Jung et al. 2010, QJRM, 136, 1145.
- Kinter et al. 2011 (submitted)
- Miura et al. 2007, Sciience, 318, 1763.
- Noda et al. 2010, Atms.Res. doi: 10.1016/j.atmosres.2009.05.007.
- Oouchi et al. 2009, GRL, doi:10.1029/2009GL038271.
- Satoh et al. 2008, JCP, 227, 3486.
- Satoh et al. 2011 (in revision)
- Sekiguchi and Nakajima 2008, JQSRT, 109, 2779.
- Shukla et al. 2009, BAMS, 90, 16.
- Takata et al. 2003, GPC, 38, 209.
- Taniguchi et al. 2010, JMSJ, 88 , 571.
- Tomita and Satoh 2004, FDR, 34, 357.

Next Generation Climate Model